Colloids and Surfaces B: Biointerfaces xxx (xxxx) xxxx

Contents lists available at ScienceDirect

Colloids and Surfaces B: Biointerfaces

journal homepage: www.elsevier.com/locate/colsurfb

Mimicking biological process to detect alkaline phosphatase activity using the vitamin B_6 cofactor conjugated bovine serum albumin capped CdS quantum dots

Yachana Upadhyay[a], Shilpa Bothra[a], Rajender Kumar[a], Ashok Kumar SK[b], Suban K Sahoo[a,*]

[a] Department of Applied Chemistry, SV National Institute of Technology (SVNIT), Surat, 395007, India
[b] Materials Chemistry Division, School of Advanced Sciences, VIT University, Vellore, 632014, India

ARTICLE INFO

Keywords:
Alkaline phosphatase
Fluorescent sensor
Vitamin B6 cofactors
Quantum dots

ABSTRACT

This manuscript presents a novel bioanalytical approach for the selective ratiometric fluorescent sensing of enzymatic activity of the alkaline phosphatase (ALP) in the biological samples. The probe was designed by conjugating the pyridoxal 5′-phosphate (PLP) over the surface of bovine serum albumin (BSA) stabilized CdS quantum dots (QDs) through the interaction of free amine present in BSA with the aldehyde group of PLP. The conjugation of PLP quenched the emission of QDs. Upon addition of the ALP, the emission of QDs was restored due to the dephosphorylation and the conversion of the functionalized PLP in to pyridoxal. With this probe, the ALP activity can be detected down to 0.05 U/L and also successfully applied for the detection of ALP activity in biological samples such as human serum and plasma.

1. Introduction

Alkaline phosphatase (ALP) is one of the vastly assayed enzyme due to its ubiquitous roles in numerous biological processes in human health [1]. ALP is found mainly in the intestine, liver, bone, kidney and placenta of human body. ALP mainly catalyzes the hydrolysis and transphosphorylation of phosphomonoesters [2]. The detection of ALP as biomarker had provided inexhaustible opportunities to diagnose a number of diseases associated with the human body, such as osteoblastic bone cancer, breast cancer, ovarian cancer, prostate cancers and liver tumors. Also, the ALP quantification is done for some other diseases like diabetes, hepatitis, osteomalacia, Paget's disease, heart failure, obstructive jaundice and rickets [3–5]. Therefore, there is burgeoning interest among the chemists to develop convenient and reliable assay to monitor the ALP activity in biological samples for the disease diagnosis, biomedical research and other relevant applications [6,7].

Analytical techniques such as chromatography, isotope label, colorimetric, chemiluminescence, fluorometric, surface-enhanced Raman scattering (SERS) and electrochemical etc. have been utilized for the monitoring of ALP activity [8–12]. Except the fluorometric methods, most of the other analytical approaches require complicated pre-treatment, sophisticated instruments and also lack high selectivity, specificity and sensitivity. Therefore, recent research was devoted to developing ALP selective fluorometric assays using the suitably derived organic dyes, functionalized nanoparticles, quantum dots and noble metal nanoclusters with the added analytical advantages of high sensitivity, selectivity, simplicity, less sample consumption and cost-effectiveness [13]. Most of the recent reports on ALP selective fluorescent assays were designed by using non-natural monophosphates as substrate which upon catalytic hydrolysis with ALP generates analytically useful optical response for the ALP detection and quantification. However, very less effort is made to use the naturally occurring monophosphates like pyridoxal 5′-phosphate (PLP) to develop an ALP selective assay [14]. The vitamin B_6 PLP serves as a cofactor for more than 140 enzymes in our body and participates in various kinds of enzymatic reactions like transamination, racemization and decarboxylation. Importantly, there is a unique relation between the PLP and ALP in the biological processes. The albumin-bound PLP present in the blood can't cross the cell membranes directly; instead, this complex acts as a reservoir of pyridoxal. Before entering into cells, ALP converts PLP into pyridoxal which can cross the cell membranes. Therefore, PLP can be used as a natural substrate for the designing of chemosensors for the sensing of ALP.

There is potential applications of water-soluble semiconductor quantum dots (QDs) in the field of sensing and biosensing due to their attractive optical properties of high Stokes shifts, high fluorescence quantum yields, stability against photobleaching and longer

* Corresponding author.
E-mail address: sks@chem.svnit.ac.in (S.K. Sahoo).

https://doi.org/10.1016/j.colsurfb.2019.110624
Received 9 September 2019; Received in revised form 21 October 2019; Accepted 30 October 2019

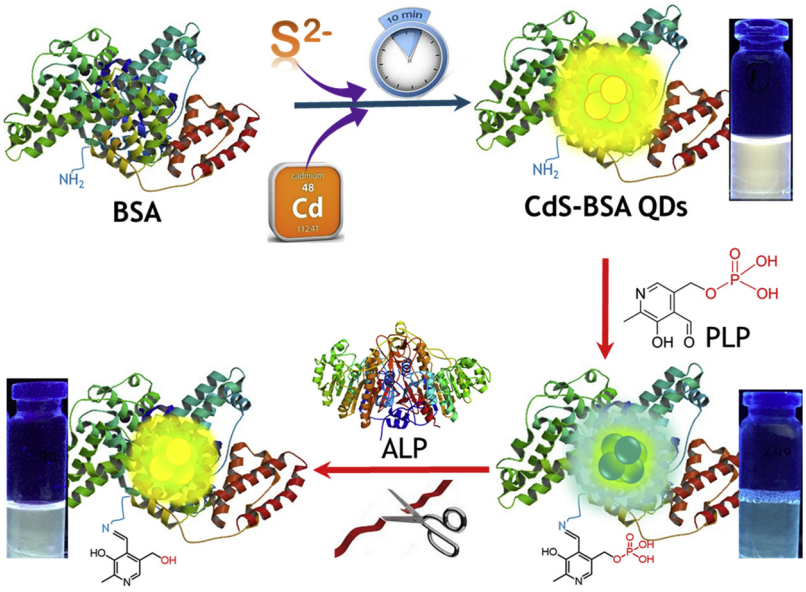

Scheme 1. Schematic diagram showing sensing mechanism of ALP activity with the PLP conjugated BSA-CdS quantum dots.

photoluminescence lifetime [15]. The biocompatibility, stability, reactivity and size-dependent emission of QDs can be easily modified by surface coating with suitable organic molecules, polymers, proteins and nucleic acids etc. Also, the cytotoxicity of QDs can be reduced remarkably after coating QDs with albumins like bovine serum albumin (BSA) and human serum albumin (HSA) [16]. As PLP can easily interact with albumin, herein, the yellow fluorescent BSA capped CdS (BSA-CdS) QDs was synthesized and investigated for the cascade fluorescent detection of the PLP and the ALP activity. As described in Scheme 1, when the vitamin B_6 cofactor is added to BSA-CdS QDs solution, the PLP selectively quenched the BSA-CdS QDs fluorescence due to the imine linkage formed between the free amine present in BSA with the aldehyde group of PLP. Subsequent addition of ALP into the PLP conjugated BSA-CdS (PLP_BSA-CdS) QDs hydrolyzed PLP and converted into pyridoxal. This hydrolysis retrieved the fluorescence intensity of QDs, which provides a straightforward bioanalytical approach for the ratiometric assay of ALP activity. Finally, the proposed method was validated by quantifying the ALP activity in human serum and plasma.

2. Experimental

2.1. Instrumentations

The instrument Cary Eclipse fluorescent spectrophotometer was used to record the fluorescence spectra (380–800 nm) whereas the UV–vis spectra (200–800 nm) were recorded by using the Varian Cary 50 spectrophotometer. Quartz cuvette of 1 cm optical path length was used to record all the spectra at room temperature. The excitation and emission slits for recording the fluorescence spectra were kept at 5 nm and 10 nm, respectively. The FT-IR spectra were measured by using the KBr pellets on a Nicolet Nexus 670 spectrometer. The quantum dots morphologies and diameter of the particles were characterized by transmission electron microscopy (TEM, Hitachi-600, and Hitachi, Japan) and the energy-dispersive X-ray spectroscopy (EDX) analysis was performed to obtain the elemental compositions of the quantum dots. The instrument Jasco Corp, J 715 Dichroism was used to study the three-dimensional structures of the BSA.

2.2. Reagents

Bovine serum albumin (BSA), adenosine triphosphate (ATP), alkaline phosphatase (ALP), adenosine diphosphate (ADP), adenosine monophosphate (AMP) and the vitamin B_6 cofactors (PLP, pyridoxal, pyridoxine and pyridoxamine) were obtained from Sigma Aldrich. The chemicals such as $CdCl_2$, NaOH, Na_2CO_3, $NaHCO_3$, $Na_2S.9H_2O$, trihydroxymethyl aminomethane (Tris), HCl and all metal salts were obtained from Rankem Pvt. Ltd., India.

2.3. Preparation of BSA-CdS QDs

The quantum dots BSA-CdS were synthesized and characterized by following the reported procedure [17,18]. Into a sample tube, 300 µL of BSA solution (2.4 mmol L^{-1}), 120 µL $CdCl_2$ solution (50 mmol L^{-1}) and 150 µL of Tris–HCl buffer (pH 8.2, 0.1 mol L^{-1}) were added and mixed thoroughly for 10 min. After that, 90 µL of Na_2S solution (30 mmol L^{-1}) was added and then diluted to 1500 µL with deionised water. The mixture was shaken carefully and equilibrated for 15 min. The formation of BSA-CdS QDs was preliminarily indicated from the color change of solution to light yellow. The synthesized BSA-CdS QDs was characterized by various techniques (UV–vis, fluorescence, FT-IR, and TEM analyses) and stored in refrigerator for further experimental studies.

2.4. Interaction of PLP with BSA-CDs

The as-prepared 100 µL of BSA-CdS QDs solution was initially diluted with 1900 µL of water, and then the different vitamin B_6 cofactors like PLP, pyridoxamine, pyridoxine and pyridoxal (200 µL, 1×10^{-3} M) were added. Then, the fluorescence spectra were recorded to investigate the selectivity of BSA-CdS QDs towards the vitamin B_6 cofactors. The fluorescence batch titration was performed by adding the different amounts of PLP (0–4.3×10^{-5} M) into the BSA-CdS QDs solution. The calibration curve was plotted using the titration data and the obtained slope was used to calculate the limit of detection (LOD) by applying the IUPAC approved equation i.e., LOD = 3 α/slope; where α is the relative standard deviation (RSD) of the fluorescence readings of the ten blank samples.

2.5. Procedure to detect ALP activity

The ALP solution was prepared by taking 1.0 mg of the enzyme in 1.0 mL carbonate buffer (pH = 10.08) to get a 1.0 mg/mL stock solution. From this stock solution, 100 µL of the ALP was taken and then

diluted to 10 mL with buffer to obtain a solution containing 0.01 mg/mL ALP. This solution was used for various spectroscopic studies. The stock solutions of other analytes (1.0 mM) were prepared freshly in double distilled water to investigate the selectivity and specificity experiments. The probe PLP_BSA-CdS solution was prepared by adding PLP (200 µL, 1×10^{-3} M) into a solution of BSA-CdS QDs which was prepared by diluting the as-prepared 100 µL of BSA-CdS QDs with 1900 µL of water. The fluorescence reading of PLP_BSA-CdS QDs in the presence of the ALP was taken after incubating the mixture for 30 min at room temperature. The fluorescence batch titration of PLP_BSA-CdS QDs was carried by adding different amounts of ALP.

2.6. Real sample analyses

The practical utility of PLP_BSA-CdS QDs was validated by detecting ALP activity in real samples such as human serum and plasma. The collected plasma and human serum samples were stored in a refrigerator for experiments. These samples are centrifuged at 10,000 rpm for 10 min and set to the neutral pH, and then diluted twice with water for spiking the standard ALP solution. After spiking of ALP to the QDs solution, the fluorescence spectra were recorded and the concentration of the ALP was estimated using the linear equation obtained from the calibration curve.

3. Results and discussion

3.1. Characterisation of BSA-CdS QDs

The analytical techniques, such as UV–vis, fluorescence, FT-IR, and TEM are applied for the characterization of yellow fluorescent BSA-CdS QDs, where the TEM image indicates the formation of spherical-shaped BSA-CdS QDs with the average diameter of ~2.74 nm estimated by considering the diameter of thirteen particles (Fig. S1). The BSA-CdS QDs showed an absorption maxima at 279 nm and an emission band centered at 520 nm (λ_{exc} = 340 nm) (Fig. S2) [17,18]. From FT-IR study (Fig. S3), the characteristics vibrational bands of the −CONH groups of BSA were observed at 1657 cm^{-1} (amide-I band), 1540 cm^{-1} (amide-II band) and 1400–1200 cm^{-1} (amide-III band) [19–23]. Also, the peak appeared around 656 cm^{-1} is an indication of the formation of Cd-S bonds [24]. Further, the EDX analysis provides information on the various elemental compositions present in the BSA-CdS QDs (Fig. S4).

3.2. Interaction of PLP with BSA-CdS QDs

The interaction between the vitamin B_6 cofactors (PLP, pyridoxal, pyridoxamine and pyridoxine) and the BSA-CdS QDs was examined by fluorescence method (Figs. 2 and S5). The cofactors pyridoxamine, pyridoxal and pyridoxine failed to perturb the emission of BSA-CdS QDs at 520 nm (λ_{exc} = 340 nm), whereas the fluorescence BSA-CdS QDs was quenched at 520 nm upon addition of PLP and a new fluorescence band appeared at 413 nm. Also, the light yellow color fluorescence of QDs solution turned to cyan blue in the presence of PLP. The kinetic study revealed that the interaction of PLP with BSA-CdS QDs along with the associated spectral changes occurred within 1 min (Fig. S6). The spectral changes is an indication of the formation of imine linkage between the −CHO group of the PLP and the free $-NH_2$ groups present in the BSA coated over the surface of BSA-CdS QDs that bring apparent conformational changes in the functionalized BSA [25]. The far-UV CD analysis of BSA-CdS QDs gave the qualitative information on the secondary structure along with the apparent conformational changes occurred during the PLP binding (Fig. S7). The BSA-CdS QDs shows two negative signals at 208 nm and 222 nm is an indication of high α-helix content of BSA in compared to β-sheet. Upon interaction with PLP, the CD spectral study revealing a decrease in the α-helix content of BSA coated over BSA-CdS QDs (Fig. S7).

The imbalance of PLP content in the human body can disrupt many important physiological processes leading to the several detrimental effects to the human health. In the United States, the patients suffering with the disease hypophosphatasia due to the low level of ALP are advised to measure the blood level of PLP. Therefore, the monitoring of PLP is important in patients facing scarcity as well as over accumulation of PLP. The high selectivity of the of BSA-CdS QDs towards PLP among the other tested vitamin B_6 cofactors encouraged us to carry out the fluorescence titration experiment by adding incremental amounts of PLP to the BSA-CdS QDs. With the successive incremental addition of PLP, there was a systematic fluorescence enhancement occurred at ~413 nm and the BSA-CdS fluorescence quenched at 520 nm (Fig. 2b), and the yellow fluorescence of BSA-CdS QDs gradually turned to cyan blue that allowed qualitative naked-eye detection of PLP (Fig. 2c). The change in fluorescence of BSA-CdS QDs showed good linear range from 0 M to 2.4×10^{-5} M for the PLP with the LOD down to 2.0 µM (Fig. S8).

3.3. Detection of ALP activity

In the biological processes, it is well known that ALP hydrolyzes PLP into pyridoxal by detaching the phosphate group from the PLP. The PLP and pyridoxal directed distinct fluorescence from the BSA-CdS QDs encourage us to biomimic the biological process of PLP hydrolysis by ALP (Fig. 1a). Accordingly, the detection of ALP activity was schematically described in Scheme 1. The yellow emission of BSA-CdS QDs is quenched by PLP but unaffected by pyridoxal. Therefore, it may be

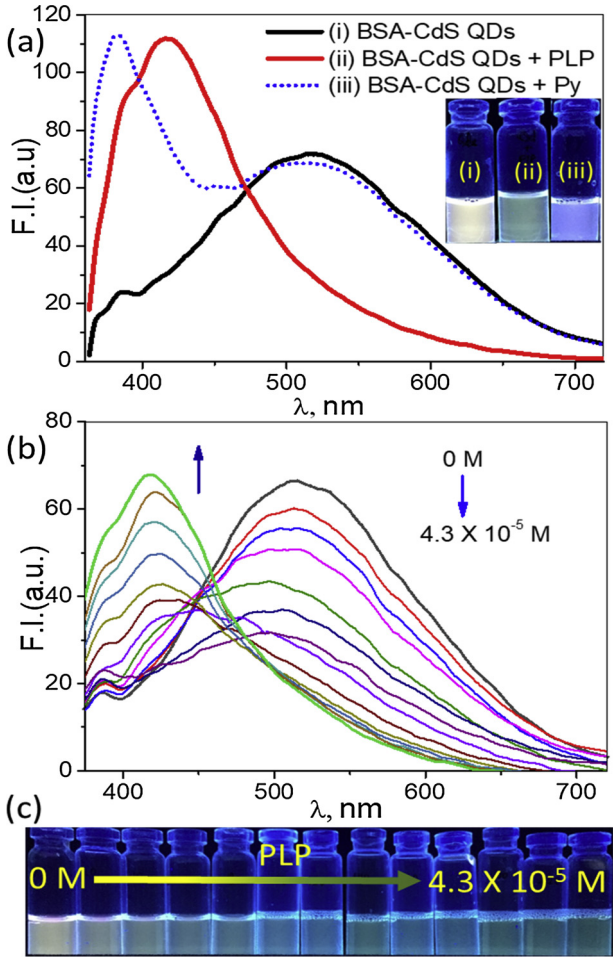

Fig. 1. (a) Fluorescence spectral changes of BSA-CdS QDs upon addition of different vitamin B_6 cofactors, (b) fluorescence titration and (c) change in the fluorescent colour (irradiated at 365 nm) of BSA-CdS QDs upon incremental addition of PLP.

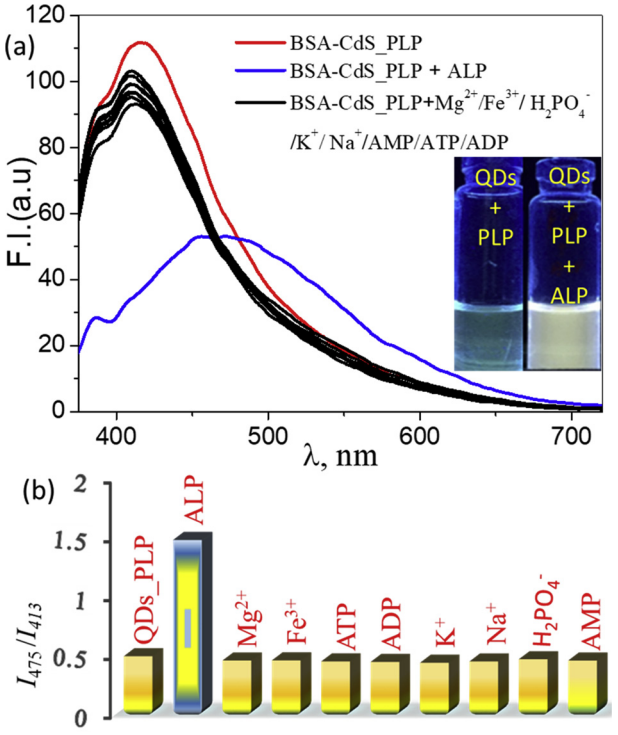

Fig. 2. (a) Fluorescence spectral changes of PLP conjugated BSA-CdS QDs and (b) the bar graph showing selectivity of the nano-assembly towards various bioactive analytes. Inset shows the fluorescent colour change of PLP conjugated BSA-CdS QDs after the addition of ALP.

expected that the addition of ALP into the PLP_BSA-CdS QDs restored the quenched emission of BSA-CdS QDs by converting PLP into pyridoxal. As the ALP activity is time dependent and also depends on the pH of the buffer solution, the experimental conditions were first optimized. Out of the various buffer solutions used (phosphate, tris and carbonate), the carbonate buffer solution with pH = 10.08 was used to study the ALP activity and also 30 min incubation time required at room temperature for the completion of the ALP activity [26].

In addition to ALP (100 µL, 0.95 U/L), other bioactive analytes (100 µL, 1×10^{-3} M), such as Mg^{2+}, Fe^{3+}, K^{+}, Na^{+}, H_2PO_4-, AMP, ADP and ATP were added to the solution of PLP_BSA-CdS QDs (1900 µL). The addition of ALP resulted in the red-shift of the fluorescence of PLP_BSA-CdS QDs with maxima at 413 nm–475 nm (Fig. 2). The fluorescent shift is an indication of the hydrolysis of PLP to pyridoxal that restored the quenched emission of BSA-CdS QDs. The undisturbed spectral nature of PLP_BSA-CdS QDs in the presence of other bioactive analytes makes this nano-assembly highly selective for the monitoring of ALP activity and therefore this probe can be applied in the complex biological samples (Fig. 2b).

The fluorescence batch titration experiment of PLP_BSA-CdS QDs was carried out by adding different amounts of ALP. For this experiment, PLP_BSA-CdS QDs (1900 µL) was taken into the several vials and different amount of ALP was added followed by diluted to 2 mL with distilled water. After incubation for 30 min, the fluorescence spectra were recorded (Fig. 3a). With the increasing amount of ALP, the fluorescence of PLP_BSA-CdS QDs at 413 nm was gradually decreased and red-shifted to 475 nm. Also, the ALP activity to hydrolyze PLP to pyridoxal can be seen by naked-eye, when observed under UV-light irradiation at 365 nm (Fig. 3b). The titration data were used to plot a calibration curve between the change in ratiometric fluorescence intensities I_{475}/I_{413} against [ALP], which showed satisfactory linearity for the detection of ALP activities in the range from 0 to 0.95 U/L (Fig. 3c). Using the slope of the calibration curve, the probe PLP_BSA-CdS QDs can be applied to detect ALP activity down to 0.05 U/L, which is better/

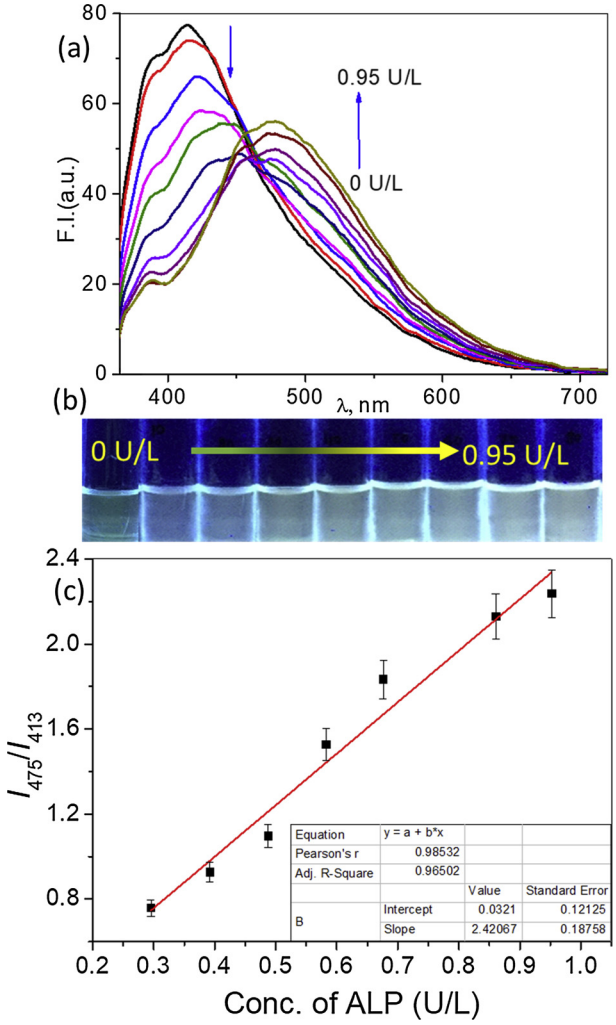

Fig. 3. (a) Binding titration and (b) naked-eye detectable fluorescent colour change of PLP conjugated BSA-CdS QDs with different amount of ALP. (c) The calibration plot of ALP (U/L) against $I_{475/413}$.

comparable with the recently reported methods (Table S1). Also, the estimated detection limit is far lower than the normal level of ALP in adults (40–190 U/L), which makes this nano-assembly useful for possible application in the detection of ALP in biological fluids [27].

To complement the practical utility of this probe PLP_BSA-CdS in complex biological samples for the quantification of ALP activity, the competitive experiment was performed (Fig. 4). For this experiment, the fluorescence of PLP_BSA-CdS QDs was recorded in the presence of ALP and the other interfering analytes mainly found in the biological samples. The bar representation of competitive experiment clearly delineated that this nanoprobe is highly specific in performing the

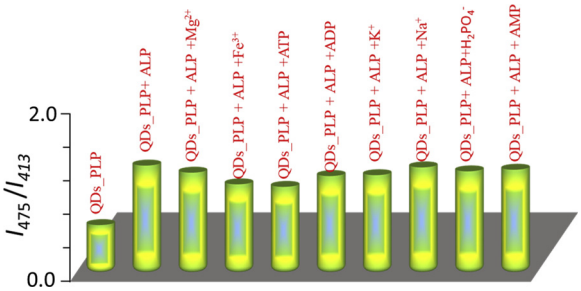

Fig. 4. Competetive experiment for the detection of ALP activity using PLP conjugated BSA-CdS QDs in the presence of other interferring analytes.

catalytic activity of ALP to hydrolyze PLP to pyridoxal even in the presence of other interfering analytes.

3.4. ALP sensing in real samples

The applicability of the developed nanoprobe was validated by quantifying ALP activity in the biological samples (human plasma and serum). The standard calculation was used to measure the recoveries of this probe PLP_BSA-CdS QDs. To get the recoveries, the human serum and plasma samples were spiked with known concentrations of ALP. After that the resulting spiked solution was added to the solution of PLP_BSA-CdS QDs and the change in fluorescence spectra were measured. Using the calibration curve, the concentration of the ALP and the percentage of recovery was estimated. As tabulated in Table S2, this nanoprobes shows satisfactory recoveries in all the tested real samples which indicating the practicability of PLP_BSA-CdS QDs for measuring the ALP activity in biological samples.

Further, a cost-effective approach was proposed for the quantification of the PLP and ALP by integrating the optical responses of quantum dots with a smartphone. Smartphone with the freely available color scanning App can measure the change in color intensity. The smartphone App record the color intensity by using the standard RGB (red, green, blue) scale. On that scale, each color ranges from 0 to 255, and the [0, 0, 0] number corresponds to absolute black whereas [255,255,255] number to true white. Using the back camera of iPhone 6 s smartphone, the fluorescent color changes of BSA-CdS QDs was monitored upon incremental addition of PLP whereas the fluorescent color changes of PLP_BSA-CdS QDs was monitored to quantify ALP. The calibration curve plotted between the R/G ratio against the added concentrations of [PLP or ALP] gave good linearity with the $R^2 > 0.95$ (Fig. S9), and the LOD was estimated down to 6.90 μM for PLP and 0.33 U/L for ALP using the nanoprobes BSA-CdS and PLP_BSA-CdS QDs, respectively.

4. Conclusions

In summary, a novel nanoprobe was developed by using BSA-CdS QDs and the PLP as monophosphate substrate for the rapid detection of ALP activity. The fluorescence of BSA-CdS QDs at 520 nm was quenched by PLP but remains unaffected in the presence of pyridoxal. Upon addition of the ALP, the functionalized PLP converted to pyridoxal followed by the emission of BSA-CdS QDs was restored. With this nanoprobe, the ALP activity can be detected down to 0.05 U/L without any noticeable interference from other tested bioactive analytes. Also, the analytical application of the probe was successfully tested for the quantification ALP activity in various real biological samples such as human plasma and serum with good recoveries. Further, we believe the simple strategy developed using the PLP and BSA-CdS QDs will give new directions for designing novel sensing systems for the detection of ALP activity and other biomolecules.

Declaration of Competing Interest

The authors declare that they have no known competing financial interests or personal relationships that could have appeared to influence the work reported in this paper.

Acknowledgements

The authors are thankful to The Director, SVNIT for necessary lab facilities and instrumental facilities. Dr Sahoo thankful to DST, New Delhi for the project grant (SR/SI/IC-54/2012).

Appendix A. Supplementary data

Supplementary material related to this article can be found, in the online version, at doi:https://doi.org/10.1016/j.colsurfb.2019.110624.

References

[1] R.B. McComb, G.N. Bowers Jr., S. Posen, Alkaline phosphatase: Springer Science & Business Media (2013).
[2] P. Song, Q. Liu, Y. Zhang, W. Liu, M. Meng, Y. Yin, et al., The chemical redox modulated switch-on fluorescence of carbon dots for probing alkaline phosphatase and its application in an immunoassay, RSC Adv. 8 (2018) 162–169.
[3] A.F. Siller, M.P. Whyte, Alkaline phosphatase: discovery and naming of our favorite enzyme, J. Bone Miner. Res. 33 (2018) 362–364.
[4] D. Shi, Y. Sun, L. Lin, C. Shi, G. Wang, X. Zhang, Naked-eye sensitive detection of alkaline phosphatase (ALP) and pyrophosphate (PPi) based on a horseradish peroxidase catalytic colorimetric system with Cu (ii), Analyst 141 (2016) 5549–5554.
[5] U. Sharma, D. Pal, R. Prasad, Alkaline phosphatase: an overview, Indian J. Clin. Biochem. 29 (2014) 269–278.
[6] H. Jiang, X. Wang, Alkaline phosphatase-responsive anodic electrochemiluminescence of CdSe nanoparticles, Anal. Chem. 84 (2012) 6986–6993.
[7] G. Li, H. Fu, X. Chen, P. Gong, G. Chen, L. Xia, et al., Facile and sensitive fluorescence sensing of alkaline phosphatase activity with photoluminescent carbon dots based on inner filter effect, Anal. Chem. 88 (2016) 2720–2726.
[8] J.-K. Min, H.-S. Yoo, E.-Y. Lee, W.-J. Lee, Y.-M. Lee, Simultaneous quantitative analysis of sphingoid base 1-phosphates in biological samples by o-phthalaldehyde precolumn derivatization after dephosphorylation with alkaline phosphatase, Anal. Biochem. 303 (2002) 167–175.
[9] F.X. Wang, C. Ye, S. Mo, L.L. Liao, X.F. Zhang, Y. Ling, et al., A novel “signal-on” photoelectrochemical sensing for ultrasensitive detection of alkaline phosphatase activity based on TiO2/g-C3N4 heterojunction, Analyst 143 (2018) 3399–3407.
[10] C. Song, C. Zhang, M.P. Zhao, Development of a high-throughput screening platform for DNA 3′-phosphatases and their inhibitors based on a universal molecular beacon and quantitative real-time PCR, Chem. Asian J. 5 (2010) 1146–1151.
[11] R. Freeman, T. Finder, R. Gill, I. Willner, Probing protein kinase (CK2) and alkaline phosphatase with CdSe/ZnS quantum dots, Nano Lett. 10 (2010) 2192–2196.
[12] W. Zhang, H. Yang, N. Li, N. Zhao, A sensitive fluorescent probe for alkaline phosphatase and an activity assay based on the aggregation-induced emission effect, RSC Adv. 8 (2018) 14995–15000.
[13] H. Liu, M. Li, Y. Xia, X. Ren, A turn-on fluorescent sensor for selective and sensitive detection of alkaline phosphatase activity with gold nanoclusters based on inner filter effect, ACS Appl. Mater. Interfaces 9 (2016) 120–126.
[14] J. Li, L. Si, J. Bao, Z. Wang, Z. Dai, Fluorescence regulation of poly (thymine)-templated copper nanoparticles via an enzyme-triggered reaction toward sensitive and selective detection of alkaline phosphatase, Anal. Chem. 89 (2017) 3681–3686.
[15] H. Liu, P. Guyot-Sionnest, Photoluminescence lifetime of lead selenide colloidal quantum dots, J. Phys. Chem. C 114 (2010) 14860–14863.
[16] R. Wojnarowska-Nowak, J. Polit, A. Zięba, I. Stolyarchuk, S. Nowak, M. Romerowicz-Misielak, et al., Colloidal quantum dots conjugated with human serum albumin–interactions and bioimaging properties, Opto-Electron. Rev. 25 (2017) 137–147.
[17] H. Matsumoto, T. Sakata, H. Mori, H. Yoneyama, Preparation of monodisperse CdS nanocrystals by size selective photocorrosion, J. Phys. Chem. 100 (1996) 13781–13785.
[18] P. Mandal, S. Talwar, S. Major, R. Srinivasa, Orange-red luminescence from Cu doped CdS nanophosphor prepared using mixed Langmuir–Blodgett multilayers, J. Chem. Phys. 128 (2008) 114703.
[19] D. Ghosh, C.N. Roy, S. Mondal, S. Kundu, S. Maiti, P.K. Bag, et al., Modulation of catalytic functionality of alkaline phosphatase induced by semiconductor quantum dots: evidence of substrate-mediated protection, RSC Adv. 6 (2016) 5024–5031.
[20] X. Bu, Y. Zhou, M. He, Z. Chen, T. Zhang, Bioinspired, direct synthesis of aqueous CdSe quantum dots for high-sensitive copper(II) ion detection, Dalton Trans. 42 (2013) 15411–15420.
[21] L. Yang, R. Xing, Q. Shen, K. Jiang, F. Ye, J. Wang, et al., Fabrication of protein-conjugated silver sulfide nanorods in the bovine serum albumin solution, J. Phys Chem B 110 (2006) 10534–10539.
[22] Q. Wang, F. Ye, T. Fang, W. Niu, P. Liu, X. Min, et al., Bovine serum albumin-directed synthesis of biocompatible CdSe quantum dots and bacteria labeling, J. Colloid Interface Sci. 355 (2011) 9–14.
[23] S. Liu, F. Shi, L. Chen, X. Su, Bovine serum albumin coated CuInS2 quantum dots as a near-infrared fluorescence probe for 2, 4, 6-trinitrophenol detection, Talanta 116 (2013) 870–875.
[24] W. Na, X. Liu, S. Pang, X. Su, Highly sensitive detection of 2, 4, 6-trinitrophenol (TNP) based on lysozyme capped CdS quantum dots, RSC Adv. 5 (2015) 51428–51434.
[25] M.L. Fonda, C. Trauss, U.M. Guempel, The binding of pyridoxal 5′-phosphate to human serum albumin, Arch. Biochem. Biophys. 288 (1991) 79–86.
[26] P.L. Urban, D.M. Goodall, N.C. Bruce, Enzymatic microreactors in chemical analysis and kinetic studies, Biotechnol. Adv. 24 (2006) 42–57.
[27] L. Riancho-Zarrabeitia, M. García-Unzueta, J.A. Tenorio, J.A. Gómez-Gerique, V.L.R. Pérez, K.E. Heath, et al., Clinical, biochemical and genetic spectrum of low alkaline phosphatase levels in adults, Eur J Internal med 29 (2016) 40–45.